THE JOURNAL OF PHYSICAL CHEMISTRY C

ARTICLE

pubs.acs.org/JPCC

Atomic-Scale Field-Effect Transistor as a Thermoelectric Power Generator and Self-Powered Device

Yu-Shen Liu, Hsuan-Te Yao, and Yu-Chang Chen*

Department of Electrophysics, National Chiao Tung University, 1001 Ta Hsueh Road, Hsinchu 30010, Taiwan

ABSTRACT: Using first-principles approaches, we have investigated the thermoelectric properties and energy conversion efficiency of the paired metal−Br−Al junction. Owing to the narrow states in the vicinity of the chemical potential, the nanojunction has large Seebeck coefficients such that it can be considered an efficient thermoelectric power generator. We also consider the nanojunction in a three-terminal geometry, where the current, voltage, power, and efficiency can be efficiently modulated by the gate voltages. Such current−voltage characteristics could be useful in the design of nanoscale electronic devices such as a transistor or switch. Notably, the nanojunction as a transistor with a fixed finite temperature difference between electrodes can power itself using the Seebeck effect.

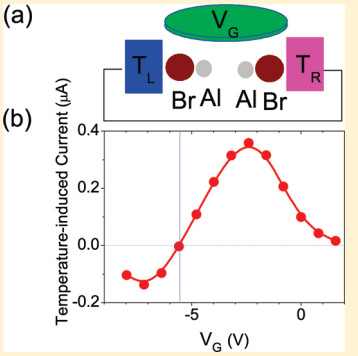

1. INTRODUCTION

In the past decade, considerable concern has arisen regarding the transport properties of atomic-scale junctions, which are the basic building blocks for molecular electronics.[1,2] This concern is motivated by the aspiration to develop new forms of electronic devices based on subminiature structures and by to understand the fundamental properties of electron transport under nonequilibrium conditions.[3] A growing number of research studies are now available to diversify the scope of electron-transport properties in molecular/atomic junctions, including current−voltage characteristics,[4−6] inelastic electron tunneling spectroscopy (IETS),[7−16] shot noise,[17−20] counting statistics,[21] local heating,[22,23] and gate-controlled effects.[24−28] Substantial progress in experiment and theory has been achieved.[29−31]

The thermoelectric effect converts thermal energy into electric energy and vice versa. A thermoelectric power generator employs the Seebeck effect to create a voltage from the difference in temperature on the two sides of the device. Recently, growing attention has been paid to the thermopower of nanojunctions. Pioneering experiments were conducted to measure the Seebeck coefficients at the atomic and molecular levels.[32−35] The Seebeck coefficient is related not only to the magnitude but also to the slope of the transmission function in the vicinity of chemical potentials. Thus, it can provide richer information than the current−voltage characteristics regarding the electronic structures of the molecule bridging the electrodes.[36]

The thermoelectric effect hybridizes the electron and energy transport, which complicates the fundamental understanding of the quantum transport of electrons and energy under nonequilibrium conditions. This has spurred rapid developments in the fundamental thermoelectric theory in nanojunctions.[37−48] Compared to certain systems with significantly enhanced Seebeck coefficients due to phonon drag,[49] effects of electron−vibration interactions on the Seebeck coefficient are weak because of quasiballistic transport in nanojunctions.[50−52] However, the current-induced dynamics with nuclear degrees of freedom of molecules provides deep insight into interactions between electrons and molecular vibrations. This subject is important and interesting because inelastic effects are efficient tools for exploring single-molecule signatures from quantum mechanical perspectives.[53] In particular, the current-induced inelastic Seebeck coefficient is an illustration of the effects relevant to current-induced dynamics. The inelastic Seebeck coefficients could be enhanced by normal modes and further magnified by local heating.[52]

Whereas the Seebeck coefficient is typically measured under equilibrium conditions, nonequilibrium current and inelastic effects potentially offer new possibilities for engineering systems leading to enhanced thermopower.[54,55] The emergence of thermoelectric nanojunctions might also have profound implications for the design of subminiature energy-conversion devices, such as nanorefrigerators.[56−58]

Thermoelectric power generators in bulk systems employ an electron gas as the working fluid. They directly convert thermal energy into electrical energy using the Seebeck effect. Provided that a temperature difference is maintained across the device, it can generate electrical power converted from the thermal energy. In this article, we explore the energy conversion mechanism of nanojunctions. We present parameter-free first-principles calculations for a thermoelectric power generator in a truly atomic-scale system. To gain further insight into the mechanism of energy conversion, we also developed an analytical theory for it.

Received: March 5, 2011
Revised: May 11, 2011
Published: July 13, 2011

ACS Publications © 2011 American Chemical Society

Scheme 1. (a) Schematic of the Thermoelectric Junction[a] and (b) Directions of Electric Current *I* and Thermal Current *J* for $S < 0$[b]

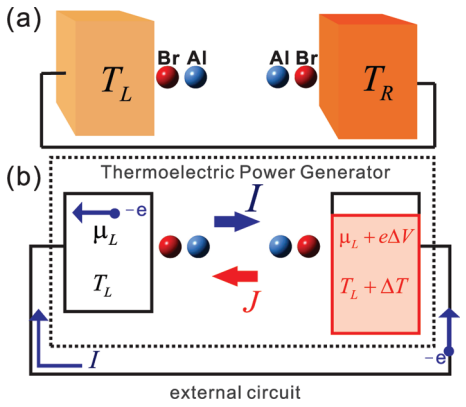

[a] Br—jellium, Al—Br, and Al—Al distance are 1.8, 4.9, and 8.6 a.u., respectively. The Al—Al distance has been significantly enlarged. [b] Inside the power generator, current travels from the lower to the higher potential, which is the opposite of what occurs when the nanojunction is a passive element in a circuit.

As a specific example, we consider the atomic junction depicted in Scheme 1a, where the left and right electrodes serve as independent cold- and hot-temperature reservoirs, respectively. This is not just an academic example because recent studies have demonstrated the capability to assemble one magnetic atom on a thin layer of atoms on the surface of a scanning tunneling microscope.[59] A similar technique might be applicable to a single Al atom adsorbed onto a layer of Br atoms on a metal surface. In this regard, the atomic junction could be formed by bringing two identical pieces of metal—Br—Al surfaces close together before the reconstruction of Br and Al atoms occurs.

As reported in ref 60, the paired metal—Br—Al junction shows interesting device properties, such as negative differential resistance, that utilize the relatively narrow density of states (DOS) near the chemical potentials. The narrow DOS is due to the weak coupling between the Al atoms and the electrodes through the "spacer" Br atoms.[61,62] This junction also serves as an efficient field-effect transistor because the narrow DOS near chemical potentials can be easily shifted by the gate voltages.

As the Seebeck coefficients are relevant to the slope of the DOS, the sharp DOS results in a large magnitude of the Seebeck coefficient.[55] The feature of a narrow DOS in the paired metal—Br—Al system comes from the increase in the distance between pairs of Al atoms. It concurrently leads to suppression of the electron transport. However, when the Al—Al distance is increased to 8.6 au, the bias-driven current at a given bias is still larger than that in typical single-molecule junctions such as the benzene 1,4-dithiolate seen in refs 60 and 63.

When a temperature difference is maintained between electrodes in a closed circuit, the Seebeck effect generates an electromotive force (emf) that drives a current flowing through the junction; hence, the nanojunction can also be considered as an efficient thermoelectric power generator.[64] We investigated further the possibility of powering an atomic-scale device as a field-effect transistor using heat instead of electricity. To illustrate this point, we considered the paired metal—Br—Al junction in a three-terminal geometry. When a finite temperature difference is maintained between electrodes, the Seebeck effect converts the electron's thermal current into electric current flowing through the nanojunction.

We observed that the current's magnitude, polarity, and on—off power are controllable by the gate field. Such current—voltage characteristics could be useful in the design of nanoscale electronic devices, such as transistors or switches. The nanojunction, therefore, can be considered a transistor that employs the Seebeck effect to power itself by converting thermal energy into electric energy. The results of this study should be of interest to researchers attempting to develop new styles of thermoelectric nanodevices.

The flow of the discussion in this paper is as follows: We describe density functional theory and the theories of thermoelectricity and thermoelectric power generation in section 2. In section 3, we discuss the thermoelectric properties of nanojunctions in an open circuit and then the thermoelectric power generator in a closed circuit. We summarize our findings in section 4.

2. THEORETICAL METHODS

We briefly present an introduction of the Lippmann—Schwinger (LS) equation and density-functional theory (DFT) in subsection 2.A. In subsection 2.B, we present the theory of Seebeck coefficient, electric conductance, and thermal conductance. In subsection 2.C, we present the theory used to calculate the Seebeck-induced electric current, voltage, power, and efficiency of energy conversion.

These quantities were calculated for the truly atomic-scale junction in terms of the nonequilibrium effective single-particle scattering wave functions obtained self-consistently in the framework of DFT + LS calculations. Both DFT + LS and DFT + Keldysh nonequilibrium Green's function (NEGF) have been applied extensively to a wide range of problems of nonequilibrium quantum transport of device physics under finite biases from first-principles approaches. It is well-known that the Lippmann—Schwinger equation and NEGF are equivalent to each other in terms of effective single-particle scattering theory in the mean-field approximation.

2.A. Density Functional Theory and the Lippmann—Schwinger Equation. We model a nanoscale junction as a passive element formed by two semi-infinite metals with planar surfaces held a fixed distance apart and connected to an external battery of bias V_B, with a nanostructured object bridging the gap between them. The full Hamiltonian of the system is $H = H_0 + V$, where H_0 is the Hamiltonian due to the biased bimetallic electrodes, modeled as an ideal metal (jellium model), and V is the scattering potential of a group of atoms bridging the gap. We assume that the left electrode is positively biased such that $V_B = (\mu_R - \mu_L)/e$, where $\mu_L = \mu$ and $\mu_R = \mu + eV_B$ are the chemical potentials deep in the left and right electrodes, respectively.

The unperturbed wave functions of the biased bimetallic electrodes have the form, $\Psi^{0,L(R)}_{E\mathbf{K}_\parallel}(\mathbf{r}) = e^{i\mathbf{K}_\parallel \cdot \mathbf{r}_\parallel} u^{L(R)}_{E\mathbf{K}_\parallel}(z)$, where $\mathbf{r}_\parallel$ is the coordinate parallel to the surfaces and z is the coordinate normal to them. Electrons are free to move in the plane perpendicular to the z direction, and $\mathbf{K}_\parallel$ is the momentum of electrons in the plane parallel to the electrode surface. Partial charges spill from the electrode positive-background edges into the vacuum region. This causes an electrostatic potential barrier between two electrodes. The charge density distribution and effective single-particle wave functions $u^{L(R)}_{E\mathbf{K}_\parallel}(z)$ are calculated in

the framework of the density functional formalism by solving the coupled Schrödinger and Poisson equations iteratively until self-consistency is obtained.[65] The wave function describes the electrons incident from the right electrode, satisfying the boundary conditions

$$u^{\mathrm{R}}_{E\mathbf{K}_\parallel}(z) = (2\pi)^{-3/2} \times \begin{cases} \frac{1}{\sqrt{k_{\mathrm{R}}}}(e^{-ik_{\mathrm{R}}z} + Re^{ik_{\mathrm{R}}z}) & z \to \infty \\ \frac{1}{\sqrt{k_{\mathrm{L}}}}Te^{-ik_{\mathrm{L}}z} & z \to -\infty \end{cases} \quad (1)$$

The group of atoms is considered in the scattering approaches. Corresponding to each of the unperturbed wave functions, a Lippmann−Schwinger equation involving a Green's function for the biased bimetallic junction is solved in the plane-wave basis, where a basis of approximately 2300 plane waves was chosen for this study[66]

$$\Psi^{\mathrm{L(R)}}_{E\mathbf{K}_\parallel}(\mathbf{r}) = \Psi^{0,\mathrm{L(R)}}_{E\mathbf{K}_\parallel}(\mathbf{r}) + \int d^3\mathbf{r}_1 \int d^3\mathbf{r}_2\, G^0_E(\mathbf{r},\mathbf{r}_1)\, V(\mathbf{r}_1,\mathbf{r}_2)\, \Psi^{\mathrm{L(R)}}_{E\mathbf{K}_\parallel}(\mathbf{r}_2) \quad (2)$$

where $\Psi^{\mathrm{L(R)}}_{E\mathbf{K}_\parallel}(\mathbf{r})$ represents the nonequilibrium scattering wave function of the electrons with energy E incident from the left (right) electrode. The quantity G^0_E is the Green's function for the biased bimetallic electrodes, and $V(\mathbf{r}_1,\mathbf{r}_2)$ is the scattering potential experienced by the electrons, given by

$$V(\mathbf{r}_1,\mathbf{r}_2) = V_{ps}(\mathbf{r}_1,\mathbf{r}_2) + \left\{ (V_{xc}[n(\mathbf{r}_1)] - V_{xc}[n_0(\mathbf{r}_1)]) + \int d\mathbf{r}_3 \frac{\delta n(\mathbf{r}_3)}{|\mathbf{r}_1 - \mathbf{r}_3|} \right\} \delta(\mathbf{r}_1 - \mathbf{r}_2) \quad (3)$$

where $V_{\mathrm{ps}}(\mathbf{r}_1,\mathbf{r}_2)$ is the electron−ion interaction potential represented by a pseudopotential, $V_{\mathrm{xc}}[n(\mathbf{r})]$ is the exchange-correlation potential calculated at the level of the local-density approximation, $n_0(\mathbf{r})$ is the electron density for the pair of biased bare electrodes, $n(\mathbf{r})$ is the electron density for the total system, and $\delta n(\mathbf{r})$ is their difference. The wave functions of the entire system are calculated iteratively until self-consistency is obtained.[66]

These right- and left-moving wave functions, weighted with the Fermi−Dirac distribution function according to their energies and temperatures, are applied to calculate the electric current as

$$I(\mu_{\mathrm{L}}, T_{\mathrm{L}}; \mu_{\mathrm{R}}, T_{\mathrm{R}}) = \frac{e\hbar}{mi} \int dE \int d\mathbf{r}_\parallel \int d\mathbf{K}_\parallel \left[f_E(\mu_{\mathrm{R}}, T_{\mathrm{R}})\, I^{RR}_{EE',\mathbf{K}_\parallel}(\mathbf{r}) - f_E(\mu_{\mathrm{L}}, T_{\mathrm{L}})\, I^{LL}_{EE',\mathbf{K}_\parallel}(\mathbf{r}) \right] \quad (4)$$

where $I^{\mathrm{RR(LL)}}_{EE',\mathbf{K}_\parallel}(\mathbf{r}) = [\Psi^{\mathrm{R(L)}}_{E,\mathbf{K}_\parallel}(\mathbf{r})]\nabla\Psi^{\mathrm{R(L)}}_{E',\mathbf{K}_\parallel}(\mathbf{r}) - \nabla[\Psi^{\mathrm{R(L)}}_{E,\mathbf{K}_\parallel}(\mathbf{r})]\Psi^{\mathrm{R(L)}}_{E',\mathbf{K}_\parallel}(\mathbf{r})$ and $d\mathbf{r}_\parallel$ represents an element of the electrode surface. Here, we assume that the left and right electrodes are independent electron reservoirs, with the electron population described by the Fermi−Dirac distribution function, $f_E(\mu_{\mathrm{L(R)}}, T_{\mathrm{L(R)}}) = 1/\{\exp[(E - \mu_{\mathrm{L(R)}})/(k_{\mathrm{B}}T_{\mathrm{L(R)}})]+1\}$, where $\mu_{\mathrm{L(R)}}$ and $T_{\mathrm{L(R)}}$ are the chemical potential and the temperature in the left (right) electrode, respectively. More detailed descriptions of the theory can be found in refs 5, 66, and 69.

The above expression can be cast in a Landauer−Büttiker formalism

$$I(\mu_{\mathrm{L}}, T_{\mathrm{L}}; \mu_{\mathrm{R}}, T_{\mathrm{R}}) = \frac{2e}{h} \int dE\, \tau(E)[f_E(\mu_{\mathrm{R}}, T_{\mathrm{R}}) - f_E(\mu_{\mathrm{L}}, T_{\mathrm{L}})] \quad (5)$$

where $\tau(E) = \tau^{\mathrm{R}}(E) = \tau^{\mathrm{L}}(E)$ is a direct consequence of the time-reversal symmetry and $\tau^{\mathrm{R(L)}}(E)$ is the transmission function of an electron with energy E incident from the right (left) electrode

$$\tau^{\mathrm{R(L)}}(E) = \frac{\pi\hbar^2}{mi} \int d\mathbf{r}_\parallel \int d\mathbf{K}_\parallel\, I^{RR(LL)}_{EE',\mathbf{K}_\parallel}(\mathbf{r}) \quad (6)$$

Note that e is positive in the definition of eq 5.

The electron's thermal current, defined as the rate at which thermal energy flows from the right (into the left) electrode, is

$$J^{\mathrm{R(L)}}_{el}(\mu_{\mathrm{L}}, T_{\mathrm{L}}; \mu_{\mathrm{R}}, T_{\mathrm{R}}) = \frac{2}{h} \int dE\, (E - \mu_{\mathrm{R(L)}})\tau(E)[f_E(\mu_{\mathrm{R}}, T_{\mathrm{R}}) - f_E(\mu_{\mathrm{L}}, T_{\mathrm{L}})] \quad (7)$$

For weakly coupled systems, such as a molecule weakly adsorbed to electrodes, self-interaction errors can be significant.[67] A more elaborate consideration of exchange-correlation energies is important in providing accurate quantitative descriptions in molecular transport calculations. For strongly coupled systems, such as monatomic chains in this study, the exchange correlation in local-density approximations, which neglect dynamic corrections, is remarkably successful when compared with the experimental results.[68]

2.B. Theory of the Thermoelectric Properties of Nanoscale Junctions. First, we assume that the nanojunction is not connected to an external circuit, such that $\mu_{\mathrm{R}} = \mu_{\mathrm{L}} = \mu$ and $T_{\mathrm{R}} = T_{\mathrm{L}} = T$, and then we consider an infinitesimal current $[(dI)_T = I(\mu,T;\mu,T + dT)]$ induced by an infinitesimal temperature difference dT in the right electrode (i.e., $T_{\mathrm{R}} = T_{\mathrm{L}} + dT$). The Seebeck effect generates a voltage difference dV in the right electrode (i.e., $\mu_{\mathrm{R}} = \mu_{\mathrm{L}} + dV$), which drives current $[(dI)_V = I(\mu,T;\mu + edV,T)]$. The current cannot actually flow in an open circuit, so $(dI)_T$ counterbalances $(dI)_V$ [i.e., $dI = (dI)_T + (dI)_V = 0$]. The Seebeck coefficient (defined as $S = dV/dT$) can be obtained by expanding the Fermi−Dirac distribution functions in $(dI)_T$ and $(dI)_V$ to first order in dT and dV

$$S = -\frac{1}{eT}\frac{K_1(\mu,T)}{K_0(\mu,T)} \quad (8)$$

where

$$K_n(\mu,T) = -\int dE\, \tau(E)(E-\mu)^n \frac{\partial f_E(\mu,T)}{\partial E} \quad (9)$$

The Seebeck coefficient up to the lowest order in temperature is

$$S \approx \alpha T \quad (10)$$

where $\alpha = -\pi^2 k_{\mathrm{B}}{}^2[\partial\tau(\mu)/\partial E]/[3e\tau(\mu)]$.[47] Here, we have expanded $K_n(\mu,T)$ to the lowest order in temperature by using Sommerfeld expansion: $K_0 \approx \tau(\mu)$, $K_1 \approx [\pi^2 k_{\mathrm{B}}{}^2\tau'(\mu)/3]T^2$, and $K_2 \approx [\pi^2 k_{\mathrm{B}}{}^2\tau(\mu)/3]T^2$. The Seebeck coefficient is positive (negative) when the slope of the transmission function is negative (positive) near the chemical potential.

When a finite temperature difference $\Delta T = T_{\mathrm{R}} - T_{\mathrm{L}} > 0$ arises in the right electrode, the Seebeck effect generates a finite electromotive force, emf $= |\Delta V(T_{\mathrm{L}},T_{\mathrm{R}})|$, raising the potential

energy of the charge. We assume that the voltage difference, $\Delta V(T_L,T_R)$, is applied to the right electrode such that $\mu = \mu_L$ and $\mu_R = \mu_L + e\Delta V(T_L,T_R)$. The voltage difference $\Delta V(T_L,T_R)$ generated by the temperature difference ΔT is approximately given by

$$\Delta V(T_L, T_R) \approx \int_{T_L}^{T_R} S(\mu_L, T)\, dT \tag{11}$$

where the Seebeck coefficient $S(\mu,T)$ is given by eq 8 with $\mu = \mu_L$. Equation 11 becomes exact when $\Delta T \to 0$. The sign of $\Delta V(T_L,T_R)$ depends on the sign of the Seebeck coefficient $S(\mu,T)$. For example, $\Delta V(T_L,T_R) < 0$ for $S < 0$, as shown in Scheme 1b.

Equation 11 is an approximation when ΔT is finite. One must remember that the left chemical potential μ_L differs from the right chemical potential μ_R when the temperature difference ΔT is large. In this case, the Seebeck coefficient becomes relevant to both μ_L and μ_R, with a more complicated form[55]

$$S(\mu_L, T_L; \mu_R, T_R) = -\frac{1}{e}\frac{K_1(\mu_L, T_L)/T_L + K_1(\mu_R, T_R)/T_R}{K_0(\mu_L, T_L) + K_0(\mu_R, T_R)} \tag{12}$$

where $K_0(\mu_{L(R)},T_{L(R)})$ and $K_1(\mu_{L(R)},T_{L(R)})$ are given by eq 9.

Corresponding to the electric current, the extra electron's thermal current induced by an infinitesimal temperature (dT) and voltage (dV) across the junctions is

$$dJ_{el} = (dJ_{el})_T + (dJ_{el})_V \tag{13}$$

where $(dJ_{el})_T = J_{el}(\mu,T;\mu,T + dT)$ and $(dJ_{el})_V = J_{el}(\mu,T;\mu + e\,dV,T)$ can be calculated from eq 7.

The electron's thermal conductance (defined as $k_{el} = dJ_{el}/dT$) can be decomposed into two components

$$\kappa_{el}(\mu, T) = \kappa_{el}^{T}(\mu, T) + \kappa_{el}^{V}(\mu, T) \tag{14}$$

where $\kappa_{el}^{T} = (dJ_{el})_T/dT$ and $\kappa_{el}^{V} = (dJ_{el})_V/dT$. Using Sommerfeld expansion, these components can be can be written as

$$\kappa_{el}^{T}(\mu, T) = \frac{2}{h}\frac{K_2(\mu, T)}{T} \tag{15}$$

and

$$\kappa_{el}^{V}(\mu, T) = \frac{2e}{h}K_1(\mu, T)\, S(\mu, T) \tag{16}$$

where $K_1(\mu,T)$ and $K_2(\mu,T)$ are given by eq 9. One should note that $\kappa_{el}^{V} = 0$ if the Seebeck coefficient of the system is zero.

By expanding $K_n(\mu,T)$ and $S(\mu,T)$ to the lowest order in temperature, eqs 15 and 16 become

$$\kappa_{el}^{V} \approx \beta_V T^3 \quad \text{and} \quad \kappa_{el}^{T} \approx \beta_T T \tag{17}$$

where $\beta_V = -2\pi^4 k_B^4[\tau'(\mu)]^2/[9h\tau(\mu)]$ and $\beta_T = 2\pi^2 k_B^2 \tau(\mu)/3h$. In the above expansions, we have applied the Sommerfeld expansions $K_1(\mu,T) \approx [\pi^2 k_B^2 \tau'(\mu)/3]T^2$ and $K_2(\mu,T) \approx [\pi^2 k_B^2 \tau(\mu)/3]T^2$, as well as eq 10.

In the limit of zero bias, eq 5 yields the electric conductance [defined as $\sigma(T) = dI/dV$]

$$\sigma(T) = \frac{2e^2}{h}\int dE\, f_E(\mu, T)[1 - f_E(\mu, T)]\tau(E)/(k_B T) \tag{18}$$

Scheme 2. Circuit Diagram of the Thermoelectric Power Generator Depicted in Scheme 1b, Represented as an Ideal Battery with emf = V_{AB} and an Internal Resistance r[a]

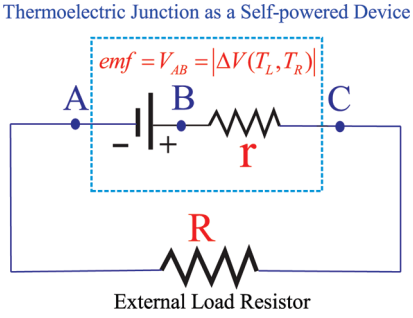

[a] We assume that no other passive elements are connected in circuit such that the external resistance is $R = 0$.

which is relatively insensitive to temperature if tunneling is the major transport mechanism.

2.C. Theory of the Thermoelectric Power Generator as a Self-Powered Electronic Device. In this subsection, we present a closed-circuit theory of the thermoelectric nanojunction as a power generator and an electronic device by itself. First, the nanojunction is considered to have a Seebeck coefficient $S < 0$. When a temperature difference $\Delta T = T_R - T_L > 0$ is applied, the thermoelectric junction employs the Seebeck effect to generate an emf = $V_{AB} = -\Delta V(T_L,T_R) > 0$ for $S < 0$, as shown in Scheme 1b. The emf drives electric current through the thermoelectric junction in a closed circuit. The thermoelectric junction as a power generator is represented as an ideal battery of emf plus an internal resistance $r = 1/\sigma$, as shown in Scheme 2. We chose clockwise as positive such that the induced current is $I > 0$ for $S < 0$.

Beginning at point A, as the current traverses the circuit in the positive direction, from Kirchhoff's loop rule, we obtain

$$V_{AB} - Ir - IR = 0 \tag{19}$$

where I is the current traversing the circuit, V_{AB} is the emf = $(\mu_R - \mu_L)/e$ of the ideal battery, r is the resistance of the nanojunction, and R is the resistance of the external resistor.

The current I encounters a potential increase due to the source of emf between points A and B, a potential drop ($V_{BC} = Ir$) due to the resistance of the junction itself between points B and C, and a potential drop ($V_{CA} = IR$) as the current traverses the external resistor between points C and A. Note that V_{AC} is the terminal voltage, which depends on the external resistor and current. As soon as the thermoelectric junction begins to supply current to a circuit, its terminal voltage falls because electric power is lost in driving current against the resistance of the junction itself. As $R \to \infty$ (open-circuit limit), the terminal voltage equals the emf.

The Seebeck coefficient, Seebeck-induced emf, thermal conductance, and internal conductance ($r \approx 1/\sigma$) are fundamental physical properties of thermoelectric junctions. These quantities are irrelevant to the choice of the external classical resistor R connected in the circuit. In this research, we particularly consider $R = 0$ without loss of generality to investigate the mechanism of energy conversion. The voltage drop between points C and A becomes $V_{CA} = IR = 0$, which yields

$$V_{AB} = Ir \tag{20}$$

dx.doi.org/10.1021/jp2021243 |J. Phys. Chem. C 2011, 115, 14988–14996

In this case, the nanojunction employs the Seebeck effect to generate electric power through a temperature difference. Concurrently, the nanojunction itself consumes all of the electric power. No electric power is supplied to external circuit. This scenario simplifies the nanojunction as a closed system, which allows for an investigation of how thermal current is converted to electric current through the Seebeck effect. Such an analysis also provides insight into the device physics of thermoelectric junctions as self-powered electronic devices. The detailed theory is represented in the remaindr of this subsection.

Provided that a finite temperature difference $\Delta T = T_R - T_L > 0$ arises in the right electrode, the Seebeck effect generates a finite electromotive force, emf = $V_{AB} = |e\Delta V|$, where the voltage difference $\Delta V = (\mu_R - \mu_L)/e$ is given by eq 11 and the Seebeck coefficient $S(\mu,T)$ is given by eq 8. The sign of ΔV depends on the Seebeck coefficient $S(\mu_L,T)$.

When the thermoelectric junction is an open circuit ($R \rightarrow \infty$), the Seebeck coefficient is measured under no current; thus, the Seebeck coefficient is calculated from $(I)_{\Delta T} + (I)_{\Delta V} = 0$, as shown in the previous subsection. When the thermoelectric junction is a closed circuit with $R = 0$, the current travels from lower potential to higher potential inside the power generator; thus, the temperature-driven current remains

$$(I)_{\Delta T} = \frac{2e}{h}\int dE\, \tau(E)[f_E(\mu_L, T_L + \Delta T) - f_E(\mu_L, T_L)] \tag{21}$$

whereas the voltage-induced current becomes

$$(I)_{\Delta V} = -\frac{2e}{h}\int dE\, \tau(E)[f_E(\mu_L + e\Delta V(T_L, T_R), T_L) - f_E(\mu_L, T_L)] \tag{22}$$

where the negative sign in front of the integral is due to the fact that current flows from lower to higher potential inside the battery (or equivalently, because $V_{BC} = -V_{AB}$). We numerically verified that $I = (I)_{\Delta V} = (I)_{\Delta T}$. $(I)_{\Delta T}$ can be interpreted as the current that traverses the thermoelectric nanojunction as a "pure" source of emf. Similarly, $(I)_{\Delta V}$ is the current that traverses the nanojunction as an internal resistor.

Equations 22 and 21 describe the flow of electrons associated with the probability flux. The flow of probability density can also transport energy. An electron with energy E that travels from the right (left) electrode carries an amount of energy $E - \mu_{R(L)}$. Correspondingly, the ΔV-induced energy currents associated with the probability current flowing out of the right electrode (into the left electrode) are

$$(J_{el}^{R(L)})_{\Delta V} = -\frac{2}{h}\int dE\, (E-\mu_{R(L)})\tau(E)[f_E(\mu_L + e\Delta V(T_L, T_R), T_L) - f_E(\mu_L, T_L)] \tag{23}$$

and the ΔT-induced energy current is

$$(J_{el})_{\Delta T} = \frac{2}{h}\int dE\, (E-\mu_L)\tau(E)[f_E(\mu_L, T_L + \Delta T) - f_E(\mu_L, T_L)] \tag{24}$$

where $\mu_R = \mu_L + e\Delta V(T_L,T_R)$ and $\Delta V(T_L,T_R)$ is given by eq 11. The sign convention defined in eqs 22−24 complies with the direction depicted in Schemes 1b and 2 for $S < 0$. Note that $(J_{el}^R)_{\Delta V}$ and $(J_{el}^L)_{\Delta V}$ are positive and $(J_{el}^R)_{\Delta V} > (J_{el}^L)_{\Delta V}$ for $S < 0$.

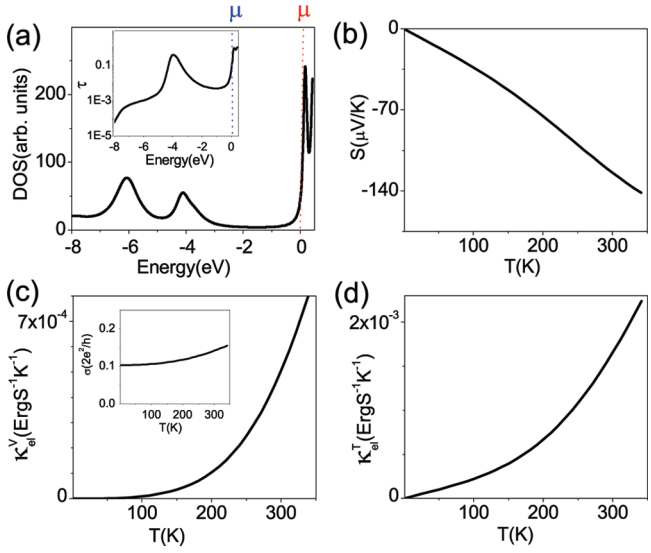

Figure 1. (a) DOS (inset: transmission function) as a function of energy. (b) Seebeck coefficient S, (c) thermal conductance induced by the temperature difference (κ_{el}^V) (inset: conductance σ), and (d) thermal conductance induced by the voltage difference (κ_{el}^T) as functions of temperature.

Subtracting $(J_{el}^L)_{\Delta V}$ from $(J_{el}^R)_{\Delta V}$, we obtain

$$\Delta P = (J_{el}^R)_{\Delta V} - (J_{el}^L)_{\Delta V} = -\Delta V(\Delta I)_{\Delta V} > 0 \tag{25}$$

where ΔP is the electric power delivered by the thermoelectric junction. It employs the Seebeck effect to convert the electron's thermal current $[(J_{el}^R)_{\Delta V} - (J_{el}^L)_{\Delta V}]$ into electric power $[-\Delta V(\Delta I)_{\Delta V}]$ through the ideal battery.

As $R \rightarrow 0$, the junction itself simultaneously consumes the entire electric power

$$\Delta P \approx \sigma(\Delta V)^2 \approx \int_{T_L}^{T_R} S\, dT \int_{T_L}^{T_R} S\sigma\, dT \tag{26}$$

Note that eq 26 can alternatively be expressed as

$$\Delta P = -\Delta V(T_L, T_R)\, I(T_L, T_R) > 0 \tag{27}$$

for $S < 0$. Equations 25−27 have been numerically verified to be consistent with each other.

If the system is n-type (i.e., $S < 0$), then $\Delta V(T_L,T_R) < 0$ and $I(T_L,T_R) > 0$, as shown in Scheme 1b. Similarly, if the system is p-type (i.e., $S > 0$), then $\Delta V(T_L,T_R) > 0$ and $I(T_L,T_R) < 0$. Both cases render $\Delta P > 0$.

In the presence of a nonzero external resistance R, the current I in the circuit can be calculated by Kirchhoff's rule (eq 19). The output electric power provided by the ideal battery can be trivially calculated as IV_{AB}.

3. RESULTS AND DISCUSSION

Provided that a finite temperature difference is raised between electrodes, the Seebeck effect will generate an electric current. It is observed that the nanojunction itself can be deemed a field-effect transistor, where the gate field can control the current.

As a specific example, we consider an atomic-scale junction in a three-terminal geometry as a thermoelectric power generator, depicted in Figure 3a. In the paired metal−Br−Al junction, we assume that the distance between two Al atoms is sufficiently

large. The interaction between two pieces of metal−Br−Al is minimal, and in this fashion, no rearrangement of atom positions occurs. Accordingly, the phonon's thermal current could be suppressed because of poor mechanical coupling between the two pieces of metal−Br−Al. We neglect this current for simplicity in this study.

3.A. Thermoelectric Properties of the Junction. In an open circuit, an infinitesimal temperature dT in the right electrode induces $(dI)_T$ and $(dI)_V$, which counterbalance each other. This gives rise to the Seebeck coefficient defined in eq 8, as described in subsection 2.B.

Correspondingly, the electron's thermal conductance is defined as $\kappa_{el} = dJ_{el}/dT$, as given by eq 14. The electron's thermal conductance can be decomposed into two components, $\kappa_{el} = \kappa_{el}^T + \kappa_{el}^V$, where κ_{el}^T and κ_{el}^V are given by eqs 15 and 16, respectively.

Figure 1a shows that the system is characterized by a sharp transmission function corresponding to a narrow DOS near the chemical potential. As reported in ref 60, the DOS becomes narrower when the distance between two Al atoms increases. The narrow DOS results in substantial Seebeck coefficients, as shown in Figure 1b. This shows that the thermoelectric junction is n-type ($S < 0$), as the narrow DOS is slightly above the chemical potential and the slope of the transmission $\tau'(\mu)$ is positive. At low temperatures (about $T < 100$ K), the Seebeck coefficients remain linear ($S \approx \alpha T$), as described in eq 10. We present the absolute values of κ_{el}^T and κ_{el}^V as functions of temperature in parts c and d, respectively, of Figure 1. At low temperatures, $\kappa_{el}^V \approx -\beta_V T^3$ and $\kappa_{el}^T \approx \beta_T T$, as shown in eq 17. The inset of Figure 1c shows the zero-bias electric conductance as a function of temperature calculated from eq 18.

3.B. The Junction as a Thermoelectric Power Generator and a Self-Powered Electronic Device. Suppose that the junction is not connected to a battery (i.e., $\mu_R = \mu_L = \mu$) and $T_R = T_L = T$. Provided that a finite temperature difference, $\Delta T = T_R - T_L$, arises in the right electrode (i.e., $T_L = T$ and $T_R = T + \Delta T$), the Seebeck effect generates a finite electromotive force emf $= |\Delta V(T_L,T_R)|$, where $\Delta V(T_L,T_R)$ is given by eq 11. This voltage difference induces a net electric current $I(T_L,T_R)$, which travels from lower to higher potential inside the power generator, as described in eq 22 and Scheme 1b.

Correspondingly, the electron's thermal current $(J_{el}^R)_{\Delta V}$ (eq 23) absorbs energy in heat from the hot (right) electrode, produces electric power ΔP (eq 25) using the Seebeck effect, and then gives up energy in heat to the cold (left) electrode through $(J_{el}^L)_{\Delta V}$ (eq 23), as described in Scheme 1b for $S < 0$.

To gain further insight into the mechanism of energy conversion, we theoretically analyze the electron's thermal current. Applying Sommerfeld expansion to $(J_{el}^R)_{\Delta V}$ and $(J_{el}^L)_{\Delta V}$ in eq 23, we obtain

$$(J_{el}^R)_{\Delta V} \approx \sigma(\Delta V)^2 T/\Delta T + \sigma(\Delta V)^2/2 \quad (28)$$

and

$$(J_{el}^L)_{\Delta V} \approx \sigma(\Delta V)^2 T/\Delta T - \sigma(\Delta V)^2/2 \quad (29)$$

where we have simplified eq 28 (and eq 29) using the following approximations: $\tau(\mu + e\Delta V) \approx \tau(\mu)$, $\tau'(\mu + e\Delta V) \approx \tau'(\mu)$, $\sigma \approx 2e^2\tau(\mu)/h$, $S \approx -\pi^2 k_B^2[\partial\tau(\mu)/\partial E]T/[3e\tau(\mu)]$, and $\Delta V \approx S\Delta T$.

Equations 28 and 29 immediately provide the law of energy conservation as further described below. The thermoelectric junction serves as an ideal source of emf that delivers electric power $\Delta P = (J_{el}^R)_{\Delta V} - (J_{el}^L)_{\Delta V}$ converted from the electron's thermal currents using the Seebeck effect. Concurrently, the nanojunction itself serves as a passive element that consumes electric power dissipated by the internal resistor at a rate of $\sigma(\Delta V^2)$.

Scheme 3. Schematic Representations of the Power Generator for (a) $(J_{el}^L)_{\Delta V} > 0$ and (b) $(J_{el}^L)_{\Delta V} < 0$[a]

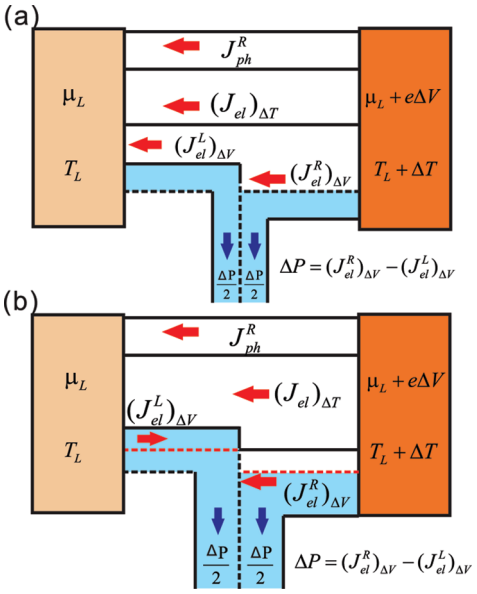

[a] Each electrode provides one-half of the electric power, $\Delta P = (J_{el}^R)_{\Delta V} - (J_{el}^L)_{\Delta V}$, using the Seebeck effect. The thermal currents J_{ph}^R and $(J_{el})_{\Delta T}$ are driven by the temperature difference ΔT, and both are not converted into electric energy.

Equations 28 and 29 imply that each electrode provides approximately one-half of the electric power using the Seebeck effect and the electric power is mainly converted from $(J_{el})_{\Delta V}$. No energy conversion is possible when the Seebeck coefficient is vanishingly small because $(J_{el}^R)_{\Delta V} = 0$. We note that $J_{el}^R = (J_{el}^R)_{\Delta V} + (J_{el})_{\Delta T}$ removes heat energy from the hot electrode, converts heat energy into electric energy, and rejects waste heat to the cold electrode by J_{el}^L. Neither $(J_{el})_{\Delta T}$ nor J_{ph}^R plays an active role in the energy conversion. The above discussions are summarized in Scheme 3a.

The energy current $(J_{el}^L)_{\Delta V}$ flowing into the cold electrode could be negative when ΔT is sufficiently large, as shown in Scheme 3b. To show this, we integrate eq 11 using eq 10, $K_1(\mu,T) \approx [\pi^2 k_B^2 \tau'(\mu)/3]T^2$, and $K_2(\mu,T) \approx [\pi^2 k_B^2 \tau(\mu)/3]T^2$. We obtain $\Delta V \approx \alpha T^2[(\Delta T/T)^2 + 2(\Delta T/T)]/2$, where $\alpha = -\{\pi^2 k_B^2[\partial\tau(\mu)/\partial E]/[3e\tau(\mu)]\}$. Together with eq 29, we arrive at

$$(J_{el}^L)_{\Delta V} \approx \sigma S T \Delta V\{1 - [(\Delta T/T) + (\Delta T/T)^2]/4\} \quad (30)$$

from which we observe that $(J_{el}^L)_{\Delta V}$ changes sign at $\Delta T \approx 1.236T$ (which is universal) and $(J_{el}^L)_{\Delta V} < 0$ for $\Delta T \gtrsim 1.236T$. Scheme 3 illustrates the schematic representation of energy conversion for both positive and negative values of $(J_{el}^L)_{\Delta V}$.

We now focus on the energy conversion efficiency, η_{el}, defined as the ratio of the electric power ΔP generated by the Seebeck effect to the electron's thermal current, $J_{el}^R = (J_{el}^R)_{\Delta V} + (J_{el})_{\Delta T}$, which removes thermal energy from the high-temperature reservoir

$$\eta_{el} = \frac{\Delta P}{J_{el}^R} \quad (31)$$

dx.doi.org/10.1021/jp2021243 |J. Phys. Chem. C 2011, 115, 14988–14996

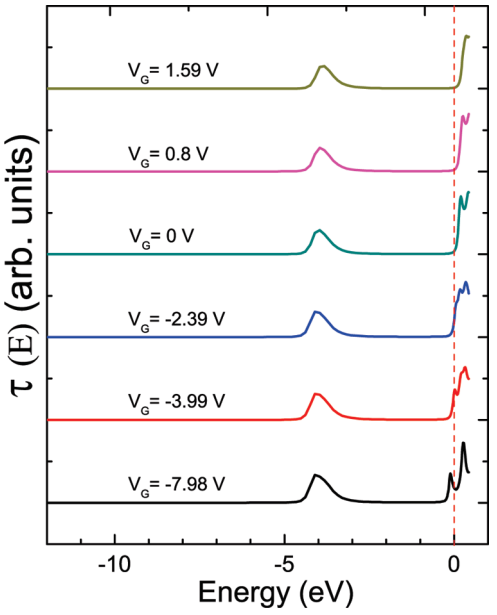

Figure 2. Transmission function as a functions of energy for various gate voltages (V_G, as indicated. The Fermi level is set as the zero of energy.

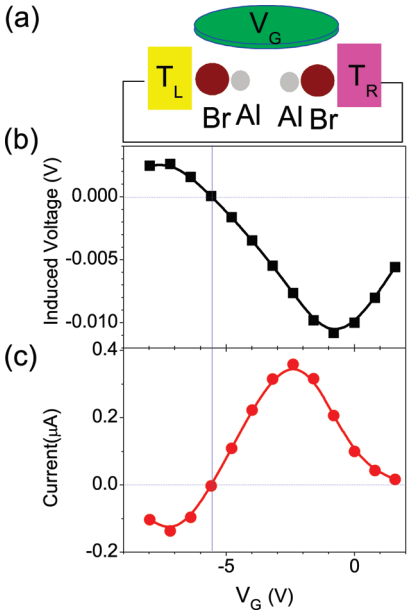

Figure 3. (a) Schematic of the three-terminal junction. Seebeck-effect-induced (b) voltage $V(T_L,T_R)$ and (c) current $I(T_L,T_R)$ as functions of gate voltage through the temperature difference $\Delta T = T_R - T_L$, where T_L = 200 K and T_R = 300 K.

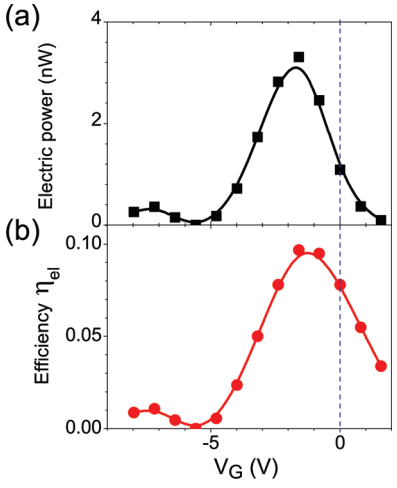

Figure 4. (a) Electric power, ΔP, converted from the thermal energy using the Seebeck effect, as a function of the gate voltage. (b) Corresponding efficiency of energy conversion η_{el} versus V_G. The temperatures of the electrodes were maintained at T_L = 200 K and T_R = 300 K.

where ΔP, $(J_{el}^R)_{\Delta V}$, and $(J_{el})_{\Delta T}$ are given by eqs 27, 23, and 24, respectively. In the above definition, we have neglected other effects (e.g., the phonon's thermal current J_{ph}^R and possible photon radiation) that transfer energy from the hot to the cold electrode.

From this viewpoint, the energy conversion efficiency presented in this study might be overestimated. We note that the size of the paired metal—Br—Al system is small. This could lead to suppression of the photon radiation because photon radiation is proportional the surface area. Moreover, the paired metal—Br—Al system has a poor mechanical link between electrodes when the distance between two Al atoms is sufficiently large. The poor mechanical coupling between two phonon reservoirs could lead to suppression of the phonon's thermal current. These two features are helpful for increasing the energy conversion efficiency. Note that the phonon's thermal current and photon radiation do not affect the magnitudes of the current and electric power generated by the Seebeck effect.

To show that the atomic junction can be considered as a field-effect transistor that can be self-powered, we consider the nanojunction in a three-terminal geometry with a finite temperature ΔT = 100 K maintained between electrodes (where T_L = 200 K and T_R = 300 K). The gate field is introduced as a capacitor composed of two parallel circular charged disks separated a certain distance from each other. The axis of the capacitor is perpendicular to the transport direction. One plate is placed close to the nano-object, whereas the other plate, placed far from the nano-object, is set to be the zero reference field.[24−27]

The nanojunction can be considered as a field-effect transistor that is powered by itself through the temperature difference maintained between electrodes using the Seebeck effect. We observe that the gate voltages can shift the narrow DOS and transmission function near the chemical potential, as shown in Figure 2. Figure 3 shows the induced potential $\Delta V(T_L,T_R)$ (upper panel; given by eq 11) and current $I(T_L,T_R)$ (lower panel; given by eq 22) for T_L = 200 K and T_R = 300 K as functions of the gate voltage. We observe that the extrema of $\Delta V(T_L,T_R)$ and $I(T_L,T_R)$ do not occur at the same value of V_G because the gate voltage also modulates the conductance of the junction [note that $\sigma = I(T_L,T_R)/\Delta V(T_L,T_R)$].

Figure 3 demonstrates that the gate field can efficiently control the magnitude, polarity, and on—off power of the voltage and current induced by the Seebeck effect. Such current—voltage characteristics could be useful in the design of nanoscale electronic devices such as transistors or switches. Note that the Seebeck-induced voltage and current described in Figure 3 comply with the sign convention described in Scheme 1b.

Figure 4 shows the electric power ΔP (upper panel; given by eq 25) delivered by the battery and the energy conversion

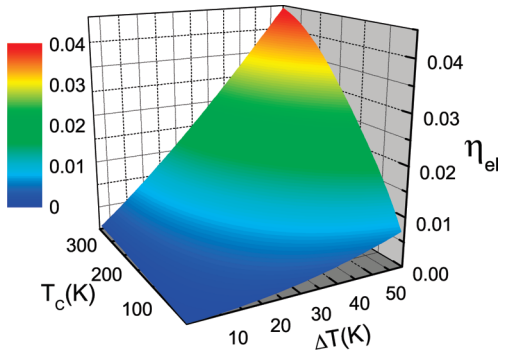

Figure 5. Efficiency of energy conversion, η_{el}, as a function of $T_L = T_C$ and $\Delta T = T_R - T_L$ for $V_G = 0$ and $R = 0$, where η_{el} was calculated using eq 31.

efficiency η_{el} (lower panel; given by eq 31) as functions of the gate voltage. It shows that the gate field is capable of controlling and optimizing the electric power and energy conversion efficiency. The energy conversion efficiency is $\eta_{el} \approx 0.09$ if optimized by the gate field. The optimized power is about 3.5 nW at $V_G \approx -2$ V. We also observe that the maximum values of electric power and energy conversion efficiency occur at different voltages, as in the case of induced voltage and current.

Finally, we investigated the efficiency of energy conversion η_{el} as a function of T_C (= T_L) and $\Delta T = T_R - T_L$ for $V_G = 0$, as shown in Figure 5. The paired metal−Br−Al junction shows sufficiently large efficiency around 0.05 when T_C = 300 K and ΔT = 60 K. Such a high efficiency is attributed to the enhanced Seebeck coefficients.

4. CONCLUSIONS

In summary, we have proposed a three-terminal nanoscale junction as a thermoelectric power generator and self-powered electronic device. We have developed theory for this device from atomistic first-principles approaches. The theory is general to any atomic/molecular junction where electron tunneling is the major transport mechanism.

As an example, we investigated the thermoelectric properties and efficiency of energy conversion of the paired metal−Br−Al junction. Owing to the narrow states near the chemical potentials, the nanojunction has large Seebeck coefficients; thus, it can be considered as an efficient thermoelectric power generator. Provided that a finite temperature difference is maintained between the electrodes, the thermoelectric junction as a power generator converts thermal energy into electric energy. The optimized electric power generated by the Seebeck effect is about 3.5 nW for T_L = 200 K and T_R = 300 K at $V_G \approx -2$ V for a single atomic chain bridging the electrodes.

To gain further insight into the mechanism of energy conversion, we investigated the electron's thermal currents analytically. The electron's thermal current that removes heat from the hot temperature reservoir can be decomposed into two components, $J_{el}^R = (J_{el}^R)_{\Delta V} + (J_{el})_{\Delta T}$. Only $(J_{el}^R)_{\Delta V}$ is capable of converting energies. The electron's thermal current removes heat from the hot reservoir through $(J_{el}^R)_{\Delta V}$ and rejects waste heat into the cold reservoir through $(J_{el}^L)_{\Delta V}$. No energy conversion is possible when the Seebeck coefficient is vanishingly small.

We also further considered the nanojunction in a three-terminal geometry. The gate field can control the magnitude, power on−off, and polarity of the induced current and voltages generated by the Seebeck effect. Such current−voltage characteristics could be useful in the design of nanoscale electronic devices such as transistors or switches. Provided that a finite temperature difference is maintained between source and drain electrodes, the thermoelectric device can generate electric power from the thermal current and drive itself as a field-effect transistor. The results of this study should be of interest to researchers attempting to develop new forms of thermoelectric nanodevices.

AUTHOR INFORMATION

Corresponding Author

*E-mail: yuchangchen@mail.nctu.edu.tw.

ACKNOWLEDGMENT

The authors thank Ministry of Education, Aiming for Top University Plan (MOE ATU), National Center for Theoretical Sciences (South), NCHC, and National Science Council (Taiwan) for support under Grants NSC 97-2112-M-009-011-MY3, 098-2811-M-009-021, and 100-2112-M-012-MY3.

REFERENCES

(1) Aviram, A.; Ratner, M. A. *Chem. Phys. Lett.* **1974**, *29*, 277.
(2) Reed, M. A.; Zhou, C.; Muller, C. J.; Burgin, T. P.; Tour, J. M. *Science* **1997**, *278*, 252.
(3) Di Ventra, M. *Electrical Transport in Nanoscale Systems*; Cambridge University Press: Cambridge, U.K., 2008.
(4) Kaun, C. C.; Guo, H. *Nano Lett.* **2003**, *3*, 1521.
(5) Di Ventra, M.; Lang, N. D. *Phys. Rev. B* **2001**, *65*, 045402.
(6) Nitzan, A.; Ratner, M. A. *Science* **2003**, *300*, 1384.
(7) Wang, W.; Lee, T.; Kretzschmar, I.; Read, M. A. *Nano Lett.* **2004**, *4*, 643.
(8) Galperin, M.; Ratner, M. A.; Nitzan, A. *Phys. Rev. B* **2008**, *78*, 125320.
(9) Jiang, J.; Kula, M.; Lu, W.; Luo, Y. *Nano Lett.* **2005**, *5*, 1551.
(10) Yu, L. H.; Zangmeister, C. D.; Kushmerick, J. G. *Phys. Rev. Lett.* **2007**, *98*, 206803.
(11) Paulsson, M.; Frederiksen, T. *Nano Lett.* **2006**, *6*, 258.
(12) Slomon, G. C.; Gagliardi, A.; Pecchia, A.; Frauenheim, T.; Di Carlo, A.; Reimers, J. R.; Noel, N. S. *J. Chem. Phys.* **2006**, *124*, 094704.
(13) Kushmerick, J. G.; Lazorcik, J.; Patterson, C. H.; Shashidhar, R. *Nano Lett.* **2004**, *4*, 639.
(14) Chen, Y. C.; Zwolak, M.; Di Ventra, M. *Nano Lett.* **2005**, *5*, 621.
(15) Chen, Y. C. *Phys. Rev. B* **2008**, *78*, 233310.
(16) Kristensen, I. S.; Paulsson, M.; Thygesen, K. S.; Jacobsen, K. W. *Phys. Rev. B* **2009**, *79*, 235411.
(17) Djukic, D.; van Ruitenbeek, J. M. *Nano Lett.* **2006**, *6*, 789.
(18) Kiguchi, M.; Tal, O.; Wohlthat, S.; Pauly, F.; Krieger, M.; Djukic, D.; Cuevas, J. C.; van Ruitenbeek, J. M. *Phys. Rev. Lett.* **2008**, *101*, 046801.
(19) Wheeler, P. J.; Russom, J. N.; Evans, K.; King, N. S.; Natelson, D. *Nano Lett.* **2010**, *10*, 1287.
(20) Chen, Y. C.; Di Ventra, M. *Phys. Rev. Lett.* **2005**, *95*, 166802.
(21) Liu, Y. S.; Chen, Y. C. *Phys. Rev. B* **2011**, *83*, 035401.
(22) Chen, Y. C.; Zwolak, M.; Di Ventra, M. *Nano Lett.* **2003**, *3*, 1691.
(23) Huang, Z.; Xu, B.; Chen, Y. C.; Di Ventra, M.; Tao, N. J. *Nano Lett.* **2006**, *6*, 1240.
(24) Di Ventra, M.; Pantelides, S. T.; Lang, N. D. *Appl. Phys. Lett.* **2000**, *76*, 3448.
(25) Ma, C. L.; Nghiem, D.; Chen, Y. C. *Appl. Phys. Lett.* **2008**, *93*, 222111.
(26) Solomon, P. M.; Lang, N. D. *ACS Nano* **2008**, *2*, 435.

(27) Lang, N. D.; Solomon, P. M. *ACS Nano* **2009**, *3*, 1437.
(28) Song, H.; Kim, Y.; Jang, Y. H.; Jeong, H.; Reed, M. A.; Lee, T. *Nature* **2009**, *462*, 1039.
(29) Ahn, C. H.; Bhattacharya, A.; Di Ventra, M.; Eckstein, J. N.; Frisbie, C. D.; Gershenson, M. E.; Goldman, A. M.; Inoue, I. H.; Mannhart, J.; Millis, A. J.; Morpurgo, A. F.; Natelson, D.; Triscone, J. M. *Rev. Mod. Phys.* **2006**, *78*, 1185.
(30) Lindsay, S. M.; Ratner, M. A. *Adv. Mater.* **2007**, *19*, 23.
(31) Tao, N. J. *Nat. Nanotechnol.* **2006**, *1*, 173.
(32) Ludoph, B.; van Ruitenbeek, J. M. *Phys. Rev. B* **1999**, *59*, 12290.
(33) Reddy, P.; Jang, S. Y.; Segalman, R. A.; Majumdar, A. *Science* **2007**, *315*, 1568.
(34) Baheti, K.; Malen, J. A.; Doak, P.; Reddy, P.; Jang, S. Y.; Tilley, T. D.; Majumdar, A.; Segalman, R. A. *Nano Lett.* **2008**, *8*, 715.
(35) Malen, J. A.; Doak, P.; Baheti, K.; Tilley, T. D.; Segalman, R. A.; Majumdar, A. *Nano Lett.* **2009**, *9*, 1164.
(36) Malen, J. A.; Yee, S. K.; Majumdar, A.; Swgalman, R. A. *Chem. Phys. Lett.* **2010**, *491*, 109.
(37) Paulsson, M.; Datta, S. *Phys. Rev. B* **2003**, *67*, 241403(R).
(38) Zheng, X.; Zheng, W.; Wei, Y.; Zeng, Z.; Wang, J. *J. Chem. Phys.* **2004**, *121*, 8537.
(39) Wang, B.; Xing, Y.; Wan, L.; Wei, Y.; Wang, J. *Phys. Rev. B* **2005**, *71*, 233406.
(40) Pauly, F.; Viljas, J. K.; Cuevas, J. C. *Phys. Rev. B* **2008**, *78*, 035315.
(41) Dubi, Y.; Di Ventra, M. *Nano Lett.* **2009**, *9*, 97.
(42) Markussen, T.; Jauho, A. P. *Phys. Rev. Lett.* **2009**, *103*, 055502.
(43) Ke, S. H.; Yang, W.; Curtarolo, S.; Baranger, H. U. *Nano Lett.* **2009**, *9*, 1011.
(44) Finch, C. M.; Garca-Suárez, V. M.; Lambert, C. J. *Phys. Rev. B* **2009**, *79*, 033405.
(45) Markussen, T.; Jauho, A. P.; Brandbyge, M. *Phys. Rev. B* **2009**, *79*, 035415.
(46) Bergfield, J. P.; Stafford, C. A. *Nano Lett.* **2009**, *9*, 3072.
(47) Liu, Y. S.; Chen, Y. R.; Chen, Y. C. *ACS Nano* **2009**, *3*, 3497.
(48) Dubi, Y.; Di Ventra, M. *Rev. Mod. Phys.* **2011**, *83*, 131.
(49) Adachi, A; Uchida, K.-I.; Saitoh, E.; Ohe, J.-I.; Takahashi, S; Maekawa, S. *Appl. Phys. Lett.* **2010**, *97*, 252506.
(50) Galperin, M.; Nitzan, A.; Ratner, M. A. *Mol. Phys.* **2008**, *106*, 397.
(51) Entin-Wohlman, O.; Imry, Y.; Aharony, A. *Phys. Rev. B* **2010**, *82*, 115314.
(52) Hsu, B. C.; Liu, Y. S.; Lin, S. H.; Chen, Y. C. *Phys. Rev. B* **2011**, *83*, 041404(R).
(53) Jorn, R.; Seideman, T. *Acc. Chem. Res.* **2010**, *43*, 1186.
(54) Esposito, M.; Lindenberg, K.; Van den Broeck, C. *Phys. Rev. Lett.* **2009**, *102*, 130602.
(55) Liu, Y. S.; Chen, Y. C. *Phys. Rev. B* **2009**, *79*, 193101.
(56) Dubi, Y.; Di Ventra, M. *Phys. Rev. B* **2009**, *79*, 081302(R).
(57) Galperin, M.; Saito, K.; Balatsky, A. V.; Nitzan, A. *Phys. Rev. B* **2009**, *80*, 115427.
(58) Liu, Y. S.; Hsu, B. C.; Chen, Y. C. *J. Phys. Chem. C* **2011**, *115*, 6111.
(59) Hirjibehedin, C. F.; Lutz, C. P.; Heinrich, A. J. *Science* **2006**, *312*, 1021.
(60) Lang, N. D. *Phys. Rev. B* **1997**, *55*, 9364.
(61) Lyo, I. M.; Avouris, Ph. *Science* **1989**, *245*, 1369.
(62) Yu, M. L.; Lang, N. D.; Hussey, B. W.; Chang, T. H. P.; Mackie, W. A. *Phys. Rev. Lett.* **1996**, *77*, 1636.
(63) Di Ventra, M.; Pantelides, S. T.; Lang, N. D. *Phys. Rev. Lett.* **2000**, *84*, 979.
(64) Bergfield, J. P.; Solis, M. A.; Stafford, C. A. *ACS Nano* **2010**, *4*, 5314.
(65) Lang, N. D. *Phys. Rev. B* **1992**, *45*, 13599.
(66) Lang, N. D. *Phys. Rev. B* **1995**, *52*, 5335.
(67) Thygesen, K. S.; Rubio, A. *Phys. Rev. B* **2008**, *77*, 115333.
(68) Sai, N.; Zwolak, M.; Vignale, G.; Di Ventra, M. *Phys. Rev. Lett.* **2005**, *94*, 186810.
(69) Chen, Y. C.; Di Ventra, M. *Phys. Rev. B* **2003**, *67*, 153304.